scientific reports

Check for updates

OPEN

Potential therapeutic effects of IL28RA inhibition on acute myocardial infarction through phosphorylated JAK1/STAT1 signaling pathways

Ge Gong[1,6], Xiangxuan Chen[2,6], Xinghu Zhang[1], Jian Yin[3,4,5]✉ & Wenhui Wan[1]✉

While current coronary intervention therapies and surgical bypass procedures are widely utilized, the treatment of acute myocardial infarction (AMI) in the elderly continues to pose significant challenges. Following AMI, the body's immune system is activated, resulting in the release of inflammatory mediators that exacerbate myocardial damage. Interleukin 28A (IL28A) and interleukin 28B (IL28B) may play a role in immune regulation post-AMI by specifically binding to interleukin 28 receptor alpha (IL28RA). However, the precise underlying mechanisms remain incompletely understood. This study aims to investigate the levels of IL28A and IL28B following AMI, as well as the protective effects of inhibiting IL28RA expression in the context of AMI and its potential mechanisms. We analyzed serum samples from 55 patients with AMI and 41 control individuals using ELISA to evaluate the levels of IL28A and IL28B, as well as to assess their correlation with the clinical parameters of the patients. Additionally, we established a mouse model of AMI and employed intramyocardial injection of lentivirus to knock down IL28RA in the myocardium. Echocardiography was utilized to compare structural and functional changes, while HE staining was conducted to analyze the infarct area and assess changes in myocardial tissue and cell morphology. The expressions of IL28A, IL28B, IL28RA, and JAK1/STAT1 pathway-related proteins in the infarct area were compared through immunofluorescence and Western blot analysis. Finally, TUNEL staining and the BAX/Bcl2 ratio were utilized to evaluate cardiomyocyte apoptosis. The study demonstrated that serum IL28A levels in patients with AMI were significantly elevated compared to those in normal controls, whereas IL28B levels were significantly reduced. Additionally, both IL28A and IL28B levels exhibit a linear relationship with high-density lipoprotein (HDL) and body mass index (BMI). In a mouse model, cardiac function deteriorated and ventricular structural changes were observed 14 days post-myocardial infarction relative to controls. The expressions of IL28A and IL28RA were significantly upregulated in the myocardium of the infarcted area, while IL28B levels showed no significant variation. Additionally, the ratios of p-JAK1/JAK1 and p-STAT1/STAT1 were significantly increased, accompanied by a notable rise in apoptotic cells within the myocardial infarction area. Importantly, the knockdown of IL28RA expression in the infarcted region effectively mitigated these alterations. These results suggest that IL28A but not IL28B contributes to the process post-AMI and may induce cardiomyocyte apoptosis through the JAK1/STAT1 pathway in conjunction with IL28RA.

Keywords IL28A, IL28B, IL28RA, Apoptosis, AMI

[1]Department of Geriatrics, Affiliated Hospital of Medical School, Jinling Hospital, Nanjing University, Nanjing 210002, China. [2]Department of Cardiology, The Affiliated Jiangning Hospital with Nanjing Medical University, Nanjing 211100, China. [3]Department of Orthopedics, The Affiliated Jiangning Hospital with Nanjing Medical University, Nanjing 211100, China. [4]Department of Orthopedics, Jiangning Clinical College of Medicine, Kangda College, Nanjing Medical University, Nanjing 211100, Jiangsu, China. [5]Department of Orthopedics, Jiangning Clinical College of Medicine, Jiangsu Institute of Health Vocational College, Nanjing 211100, Jiangsu, China. [6]Ge Gong and Xiangxuan Chen contributed equally to this work. ✉email: yinjiandoc@njmu.edu.cn; wanwhnju@163.com

nature portfolio

With changes in people's living environments and increasing social pressures, the incidence rate of acute myocardial infarction (AMI) is rising. Although current coronary intervention therapies and surgical bypass procedures are widely employed, treatment for the elderly remains challenging. Additionally, preventing and managing cardiac dysfunction following myocardial infarction has become a significant issue for clinicians. Ventricular remodeling begins within hours of AMI onset and persists throughout the chronic phase of cardiac insufficiency, playing a crucial role in its development. Therefore, a thorough investigation of the pathophysiological processes involved in ventricular remodeling after myocardial infarction, along with the exploration of more effective intervention targets, is essential for preventing and treating ventricular remodeling and improving chronic cardiac dysfunction.

Following AMI, the immune system is activated, resulting in aseptic inflammation and the release of inflammatory mediators and reactive oxygen species, which exacerbate myocardial damage and contribute to the progression of heart failure. The activation of the immune system, particularly adaptive immunity, is crucial for mediating myocardial repair and remodeling[1,2]. Adaptive immunity encompasses the activation, proliferation, and differentiation of antigen-specific T and B lymphocytes, which secrete various cytokines, including interferons, to exert biological effects. This immune response plays a significant role in the pathophysiology of AMI[3]. Interferons released by T cells upon antigen stimulation exhibit broad-spectrum antiviral, antitumor, and immune regulatory functions. Traditionally classified into IFN-α, IFN-β, and IFN-γ, a novel class of cytokines known as IFN-λ has garnered increasing attention in recent years. The human IFN-λ family comprises four functional genes: IFN-λ1, IFN-λ2, and IFN-λ3 (also referred to as IL29, IL28A, and IL28B), along with one pseudogene, IFNL4[4]. Mice possess two functional genes, IL28A and IL28B, in addition to the pseudogene IFNL4. The receptor complex for IFN-λs is a heterodimer formed by IL28RA and IL10RB. IL28RA, as a specific receptor for IFN-λ, plays a pivotal role in immune regulation across various diseases upon binding with IFN-λ.

Our previous studies have noted an upregulation of IL28RA expression in cardiomyocytes under conditions of ischemia and hypoxia. By downregulating IL28RA expression, cardiomyocyte apoptosis was effectively inhibited, offering protection against myocardial injury[5,6]. However, the precise mechanism through which IFN-λ interacts with IL28RA and induces cell damage post-AMI remains elusive. This research aims to assess IL28A/B levels in the serum of myocardial infarction patients and investigate changes in IL28A/B post-AMI. Furthermore, a mouse model of AMI with reduced IL28RA expression will be utilized to delve deeper into the specific mechanisms governing the IL28A/B and IL28RA interaction post-AMI. The findings of this study will establish a theoretical groundwork for immunotherapy targeting myocardial injury post-AMI and offer novel insights for the clinical management and treatment of heart failure.

Materials and methods
Human samples
A total of 55 patients with AMI and 41 healthy controls were selected from Jinling Hospital, Medical School of Nanjing University. According to the fourth edition of the "Global Definition of Myocardial Infarction" standards, AMI is defined as acute myocardial injury, characterized by an increase and/or decrease in serum troponin levels that exceeds the 99th percentile of the upper limit of normal reference values at least once. Additionally, there must be evidence of acute myocardial ischemia, which may include: (1) symptoms indicative of acute myocardial ischemia; (2) new ischemic changes observed on electrocardiograms; (3) the formation of pathological Q waves; (4) imaging examinations revealing new myocardial necrosis or local wall motion abnormalities consistent with an ischemic etiology; and (5) confirmation of intracoronary thrombosis through coronary angiography or intraluminal imaging, while excluding autoimmune and infectious diseases. Informed consent was obtained from all participants, and the study adhered to the principles of the Declaration of Helsinki.

The serum of all patients was within 14 days after AMI. Blood samples were collected from all participants after an overnight fast, and serum was stored at -80 °C for metabolite analysis. Socio-demographic information such as age, sex, height, weight, and medical history (including tobacco use, hypertension, and diabetes) was gathered from both the AMI and control groups.

Enzyme-linked immunosorbent assay (ELISA)
Blood samples were collected, and serum samples were obtained by centrifuging the blood samples at 3500 rpm for 10 min. The supernatant was carefully collected and immediately stored at -20 °C until further analysis. The activity levels of IL28A (YJ027398) and IL28B (YJ027397) in the serum were determined using commercially available kits (Enzyme-linked Biotechnology, Shanghai, China) following the manufacturer's instructions.

Establishment of the myocardial infarction mouse model
The experimental animals used in this study were purchased from the Animal Experiment Center of Nanjing Medical University. Male C57BL/6JNifdc mice (6–8 weeks old, weighing 20–25 g) were housed in a standard vivarium maintained at a temperature of 23 ± 2 °C. They were provided with ad libitum access to food and water throughout the duration of the experiment. All animal procedures were carried out in compliance with the National Institutes of Health Guidelines for the Care and Use of Laboratory Animals. The study protocols were approved by the Animal Ethics Committee of Jingling Hospital, Nanjing University, China.

In the AMI group, mice were anesthetized with isoflurane, and a left thoracotomy was performed using a 7–0 Prolene suture (Ethicon, Inc., Somerville, NJ, USA) to permanently ligate the left anterior descending artery (LAD). Mice in the sham group also underwent thoracotomy but did not receive LAD ligation. In the shRNA knockdown group, 3–5 μL of lentivirus was injected at three points in the myocardial infarction area following ligation. All surgeries were conducted under sterile conditions to minimize the risk of infection. The specific process is shown in Fig. 1.
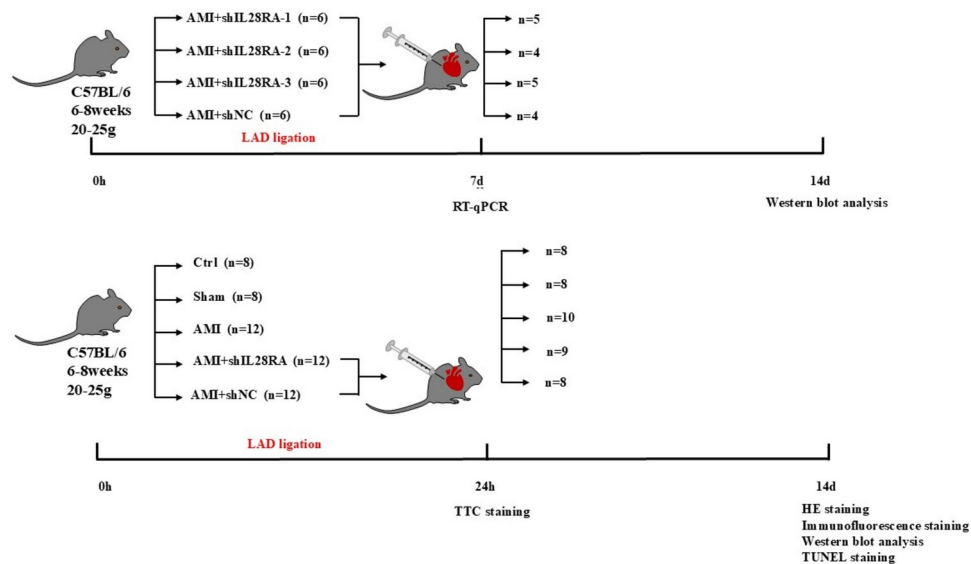
Fig. 1. A flow chart detailing the animal experiment is presented. A total of 24 male C57BL/6 mice, aged 6–8 weeks and weighing between 20 and 25 g, were utilized to establish a myocardial infarction model for the screening of IL28RA knockdown lentivirus (**A**). Subsequently, 52 C57BL/6 mice were randomly assigned to one of the following groups: (1) Ctrl group, (2) Sham group, (3) AMI group, (4) AMI + shIL28RA group, and (5) AMI + shNC group (**B**).

Cardiac structure or function detection by echocardiography

The mice were divided into five groups: normal control group, sham operation group, AMI group, AMI + shIL28RA group, and AMI + shNC group. Cardiac function was assessed in each group using a high-resolution small animal ultrasound system with a 20–23.5 MHz ultrasound probe. Ventricular wall motion was evaluated by imaging the long axis of the left ventricle and the short axis of the left ventricular papillary muscles along the left sternal border. Parameters such as left ventricular ejection fraction (EF%), left ventricular fractional shortening (FS%), left ventricular mass (LV Mass), left ventricular anterior wall thickness at end-diastole and end-systole (LVAW;d, LVAW;s), and left ventricular posterior wall thickness (LVPW;d, LVPW;s) at end-diastole and end-systole were recorded and calculated. Each measurement was taken over three cardiac cycles and averaged for subsequent analysis.

TTC staining

After 24 h of ligation, the mice were euthanized by cervical dislocation, and their hearts were promptly removed and frozen at -80 °C. The ventricular tissue was then cut into four sections perpendicular to the heart's long axis. Each heart section was individually incubated in a 24-well culture plate with a 1% triphenyl tetrazolium chloride (TTC) solution at 37 °C for 15 min, using a kit from KeyGen Biotech, Nanjing, China. Subsequently, the sections were photographed with a digital camera. Computerized planimetry was utilized to determine the infarct size areas, which were calculated as the ratio of the infarct area to the total area and expressed as a percentage. To reduce the impact of subjective factors on the experimental outcomes, the personnel responsible for conducting the TTC staining were kept unaware of the study group assignments.

HE staining

Heart tissue samples were collected on the 14th day post-surgery. Following embedding in paraffin, the tissue was sliced into 5 μm sections. Subsequently, routine dewaxing was performed, followed by staining with eosin for 2 min using the HE staining kit. The tissue was then rinsed with running water for 5 min, stained with hematoxylin for 10 min, and rinsed again for 10 min. Differentiation solution was applied for 30 s, followed by a 2-min rinse with running water. The tissue was then stained with blue-returning solution for 30 s, rinsed for 10 min, and cardiac damage post-AMI was observed after sealing.

Plasmid construction and lentivirus production

Plasmid Construction: The lentiviral vectors expressing short hairpin RNA (shRNA) targeting the sequence of IL28RA gene and a negative control (refer to Table 2) were synthesized and cloned into the GV493 (pFU-GW-016) vector with BsmBI sites (purchased from Shanghai Genechem Co., Ltd.). The recombinant vector was confirmed by DNA sequencing.

Lentivirus Production: The viral vectors were transfected into 293 T cells using Lipofectamine 2000 (Invitrogen, Thermo Fisher Scientific, Inc.) along with two helper plasmids, psPAX2 and pMD2.G. Infectious lentiviruses were harvested 72 h post-transfection, underwent rapid centrifugation to remove cell debris, and then filtered through 0.45 μm cellulose acetate filters. The virus titer was determined by fluorescence-activated

cell sorting analysis of GFP-positive 293 T cells and was approximately 1×10^9 transducing units (TU)/mL medium. The lentiviruses were stored at $-80\ °C$ for further use.

Immunofluorescence staining
Slices of mice tissues were washed with ice-cold phosphate-buffered saline (PBS), fixed in 4% paraformaldehyde, and permeabilized with 0.1% Triton X-100 in PBS for 30 min. Subsequently, the slices were blocked with 5% bovine serum albumin, followed by overnight incubation at 4 °C with primary antibodies against IL28A (YT5305, ImmunoWay, USA), IL28B (PA5-103439, Invitrogen, USA), and IL28RA (PA5-98608, Invitrogen, USA) at a dilution of 1:200. After the primary antibody incubation, the slices underwent incubation with Alexa Fluor 488-conjugated goat anti-rabbit secondary antibody (RS3211, ImmunoWay, USA) at a dilution of 1:200 for 2 h. Nuclei were stained with DAPI, and fluorescence imaging was conducted using a digital pathology slide scanner (Pannoramic 250 MIDI, 3DHISTECH, Hungary). To minimize potential bias in the experimental results, the individuals performing the immunofluorescence experiments were blinded to the MI status of the samples.

Western blot analysis
Heart tissue samples from the infarcted area were homogenized in RIPA buffer and centrifuged at 12,000 rpm for 20 min at 4 °C. The protein concentration in the supernatant was determined using the BCA method. Equal amounts of protein (36 μg) were loaded onto 6% or 10% SDS-PAGE gels for electrophoresis. The separated proteins were transferred to polyvinylidene fluoride (PVDF) membrane by electroblotting. Subsequently, the membrane was blocked with QuickBlockTM Western (Beyotime, p0252) for 20 min at 4 °C, and incubated overnight at 4 °C with primary antibodies against IL28RA (PA5-98608, Invitrogen, USA), IL28A (YT5305, ImmunoWay, USA), IL28B (PA5-103439, Invitrogen, USA), JAK1 (3344P, Cell Signaling Technology, USA), p-JAK1 (3331S, Cell Signaling Technology, USA), STAT1 (9172L, Cell Signaling Technology, USA), p-STAT1 (9167S, Cell Signaling Technology, USA), BAX(50599-2-lg, Proteintech, China) and Bcl2(26593-1-AP, Proteintech, China) at a dilution of 1:2000. After primary antibody incubation, the membranes were probed with HRP-labeled secondary antibodies (KeyGen Biotech, Nanjing, China) at a dilution of 1:10,000 for 2 h at 4 °C. The immunoblots were visualized using an ultrasensitive ECL detection reagent (Vazyme Biotech, Nanjing, China) and analyzed using ImageJ Software.

TUNEL staining
The mice ischemic myocardium was collected and fixed in a 4% paraformaldehyde solution. Myocardial apoptosis was assessed through Terminal deoxynucleotidyl transferase-mediated deoxyuridine triphosphate nick end labeling (TUNEL) staining using a Fluorescein In Situ Cell Death Detection Kit (KeyGen Biotech, Nanjing, China), following the manufacturer's instructions. Five randomly selected fields were observed per tissue slice under a digital pathology slide scanner (VS200, Olympus, Japan) to quantify the extent of cell apoptosis by calculating the ratio of TUNEL-positive nuclei to nuclei stained with DAPI. To ensure objectivity, personnel performing the TUNEL staining experiments were unaware of the myocardial infarction status of the samples.

RNA extraction, reverse transcription, and quantitative PCR (RT-qPCR)
Total RNA was extracted from the myocardium of the infarcted area in mice using Trizol (Invitrogen, CA, USA), following the manufacturer's instructions. Subsequently, the extracted RNA was reverse transcribed into cDNA using PrimeScript RT Master Mix (Vazyme, Nanjing, China). The cDNA was then quantified via SYBR green real-time PCR with 500 nM primers on QuantStudio™ 5 (Thermo Fisher), with ARPPPO serving as the reference gene. The primer sequences used for RT-qPCR as follow: Arppppo: F: GAAACTGCTGCCTCACATCCG, R: G CTGGCACAGTGACCTCACACG; IL28RA: F: CAGAAACGTGACACTCTTCTCC, R: CTGCACAATGCTC CACTGG.

Statistical analysis
All data were statistically analyzed using SPSS 22.0 software. Normally distributed data were presented as mean $\pm$ standard deviation ($\bar{x} \pm s$), and the t-test was used for comparing two groups. Non-normally distributed data were expressed as median (interquartile range), and the rank sum test was used for the comparison between two groups. The chi-squared test was applied for the analysis of count data. Differences among four groups were evaluated using one-way analysis of variance (ANOVA), followed by Tukey's post-hoc test for pairwise comparisons. Pearson correlation analysis was employed to assess the correlation between IL28A/IL28B and baseline indicators. A significance level of $P < 0.05$ was considered statistically significant. Graphs were generated using GraphPad Prism 5 software (GraphPad Software, La Jolla, CA, USA).

Results
AMI patients' characteristics and serum indicators
The study population consisted of 22 patients with AMI and 19 healthy controls. Both groups were assessed for basic characteristics such as age, gender, BMI, smoking status, hypertension, and diabetes. The analysis revealed no significant differences in age, gender, smoking, and diabetes ($P > 0.05$), but significant disparities in BMI and hypertension ($P < 0.05$) between the groups. When comparing myocardial infarction indicators like high-density lipoprotein (HDL), cardiac troponin T(cTnT), cardiac troponin I (cTnI), and creatine kinase isoenzymes (CK-MB), significant differences were noted ($P < 0.05$). Conversely, there were no statistically significant variances in triglycerides (TG), total cholesterol (TC), and low-density lipoprotein (LDL) levels between the patient and control groups. A detailed breakdown of these measurements can be found in Table 1.

	AMI (n = 55)	Control (n = 41)	P-value (AMI vs. Control)
Demographic characteristics			
Age (y)	58.42 ± 5.32	56.95 ± 8.05	0.315
Female (n)	17	8	0.208
BMI (kg/m^2)	26.67 ± 2.21	24.54 ± 1.81	0.000
Smoking (n)	19	11	0.420
Hypertension (n)	42	20	0.005
Diabetes (n)	12	4	0.117
Serum indicators			
TG (mmol/L)	4.94 ± 0.92	4.94 ± 0.86	0.994
TC (mmol/L)	1.99 ± 0.98	2.25 ± 1.17	0.249
LDL (mmol/L)	2.67 ± 0.71	2.55 ± 0.36	0.509
HDL (mmol/L)	0.92 ± 0.28	1.47 ± 0.26	0.000
cTnT (ng/ml)	0.89 ± 1.12	0.005 ± 0.001	0.000
cTnI (ng/ml)	24.26 ± 18.89	0.02 ± 0.00	0.000
CK-MB (ng/ml)	60.44 ± 46.66	10.34 ± 2.82	0.000

Table 1. Baseline and clinical characteristics of the population.
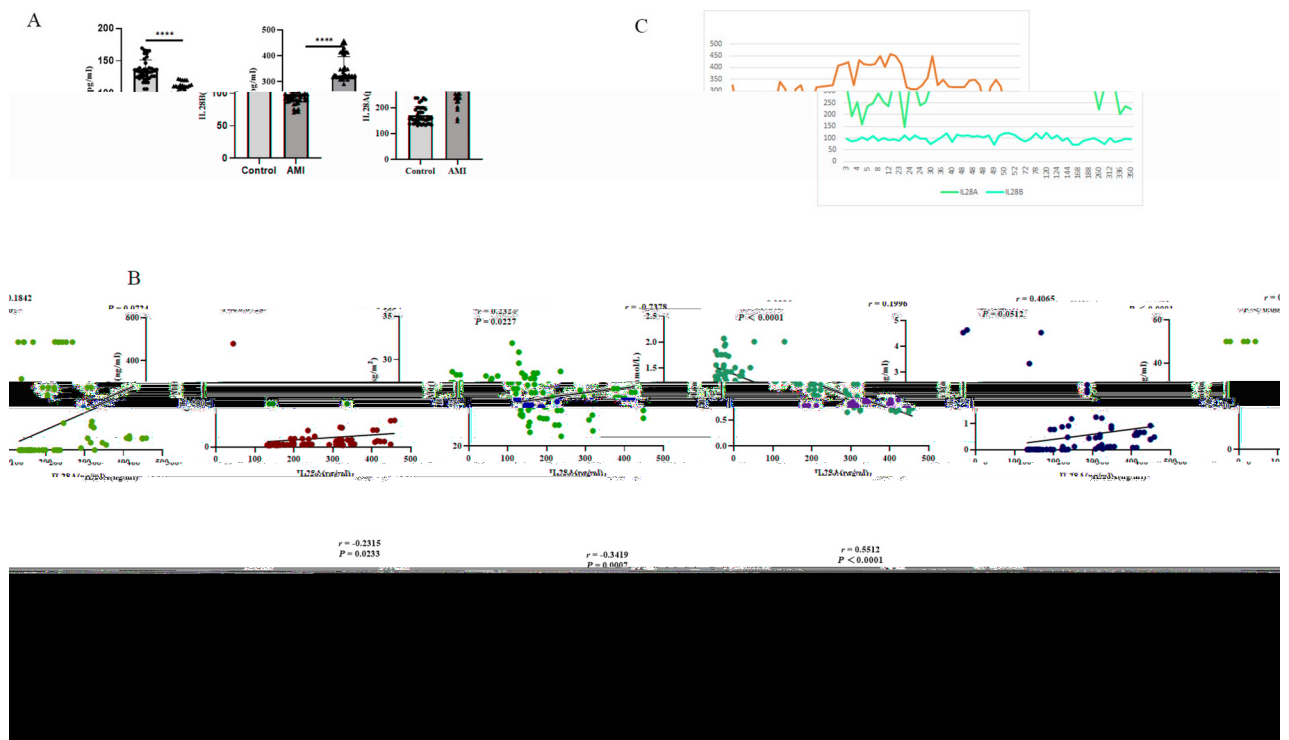
Fig. 2. This study investigates the relationship between IL28A and IL28B levels, clinical indicators, and the timing of myocardial infarction. It includes a comparison of IL28A and IL28B levels in patients who have experienced myocardial infarction versus control subjects (**A**). Additionally, it examines the correlation between IL28A and IL28B levels and various clinical parameters, including BMI, HDL, cTnT, cTnI, and CK-MB (**B**). Furthermore, the study explores the temporal changes in IL28A and IL28B levels in relation to the progression of myocardial infarction (**C**) (*$P < 0.05$, **$P < 0.01$, ****$P < 0.0001$).

Correlation between IL28A and IL28B levels and indicators in acute myocardial infarction patients

To examine changes in IL28A and IL28B levels in the serum of AMI patients, we conducted ELISA analyses to measure the concentrations of these cytokines. Our results demonstrated a notable increase in IL28A levels among AMI patients compared to the control group, while IL28B levels were significantly decreased in AMI patients relative to the control group. Interestingly, we observed that IL28A levels remained elevated from 48 to 120 h (see Fig. 2A and C).

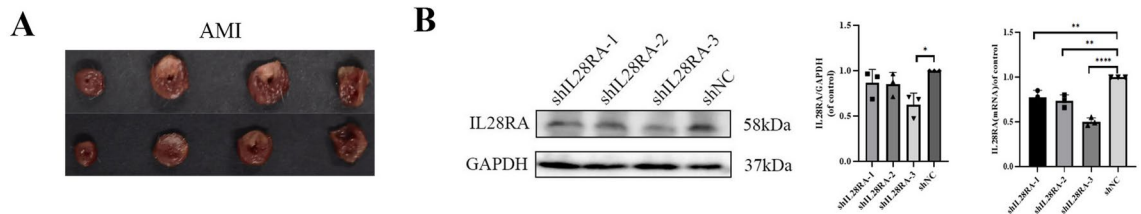| NO	Target Seq
shIL28RA-1	GACTCCTCATATAAGGATGAA
shIL28RA-2	CCCAGAAGGAACTGACCATAA
shIL28RA-3	TCCAAGTTCAAAGGACGAGTA
shNC	TTCTCCGAACGTGTCACGT

Table 2. Target sequence.

Fig. 3. The AMI model was successfully established (**A**), and the lentivirally packaged shRNA with the highest knockdown efficiency was selected. A non-targeting shRNA (shNC) served as the control, while three shRNAs were designed to target IL28RA. At the mRNA level, shIL28RA-1, shIL28RA-2, and shIL28RA-3 all demonstrated the ability to knock down IL28RA. At the protein level, only shIL28RA-3 showed a significant reduction in the protein expression of IL28RA (**B**). ($^{*}P < 0.05$, $^{**}P < 0.01$, $^{****}P < 0.0001$).

After identifying significant statistical differences in BMI, hypertension, HDL, cTnT, cTnI, and CK-MB between the AMI group and the control group, further analysis was conducted to investigate the correlation between IL28A/IL28B and these indicators. The findings revealed a negative correlation between IL28A and HDL, as well as between IL28B and BMI, cTnT, cTnI and CK-MB. Conversely, a positive correlation was observed between IL28A and BMI, cTnI, and between IL28B and HDL ($P < 0.05$) (see Fig. 2B).

IL28RA knockdown ameliorates cardiac dysfunction and tissue damage post-AMI in mice

To suppress the expression of IL28RA, three lentivirus-packaged shRNAs were designed to interfere with IL28RA expression (refer to Table 2). The lentivirus with the highest knockdown efficiency was identified using the AMI mouse model. IL28RA expression was assessed via WB and RT-qPCR, revealing that shIL28RA-3 exhibited the highest knockdown efficiency. Subsequent experiments were carried out using this specific lentivirus (see Fig. 3B and Supplementary Information 1 and 2).

The mice in the study were divided into five groups: normal control group (Ctrl), sham operation group (Sham), AMI group (AMI), AMI + shIL28RA group (AMI + shIL28RA), and AMI + shNC group (AMI + shNC). M-mode echocardiography results showed normal findings in the normal control and sham operation groups, with the heart displaying coordinated and strong contractions, and normal wall thickness. The electrocardiogram (ECG) exhibited a normal QRS wave. However, in the AMI and AMI + shNC groups, wall motion weakened, disappeared, or even reversed. The left ventricular wall showed ball-like expansion, and abnormal QRS waves and various arrhythmias were observed in the ECG (see Fig. 4A). Compared with the sham operation group, EF%, FS% and LVPWs values were significantly reduced, and LVmass was significantly increased; knocking down IL28RA expression in the myocardium could rescue these changes ($P < 0.05$). LVPWd, LVAWs and LVAWd did not show statistically significant differences among the groups ($P > 0.05$) (see Fig. 4B).

Histological analysis using HE staining on the 14th day post mouse AMI showed that the myocardial tissue in the AMI group displayed notable nuclear pyknosis, cytoplasmic dissolution, and disordered texture. Knocking down IL28RA in mice from the AMI group led to a rescue of these myocardial changes, resulting in a significant reduction in the area of myocardial tissue damage compared to the AMI group ($P < 0.05$) (see Fig. 5).

Downregulation of IL28RA Alters IL28A and IL28RA expression in the myocardium following AMI

To investigate the potential role of IL28A, IL28B, and IL28RA in regulating cardiomyocytes after AMI in an in vivo setting, we utilized an experimental AMI model. After 24 h of ligation, TTC staining was performed on the myocardial infarct area, and graphical representation of the myocardium was carried out to confirm the successful modeling of the myocardial infarction (see Fig. 3A).

Following left thoracotomy ligation for 14 days, immunofluorescence staining was conducted, revealing a significant increase in the expression of IL28A and IL28RA around the nucleus of cardiomyocytes ($P < 0.05$). However, there was no significant increase in the expression of IL28B observed (see Fig. 6). These findings suggest a potential role of IL28A and IL28RA in the regulation of cardiomyocytes following AMI.

When we downregulated IL28RA expression in the myocardial infarction area, we observed a significant reduction in the expression of IL28A and IL28RA compared to the AMI + shNC group. However, there was no significant change in the expression of IL28B (see Fig. 6).
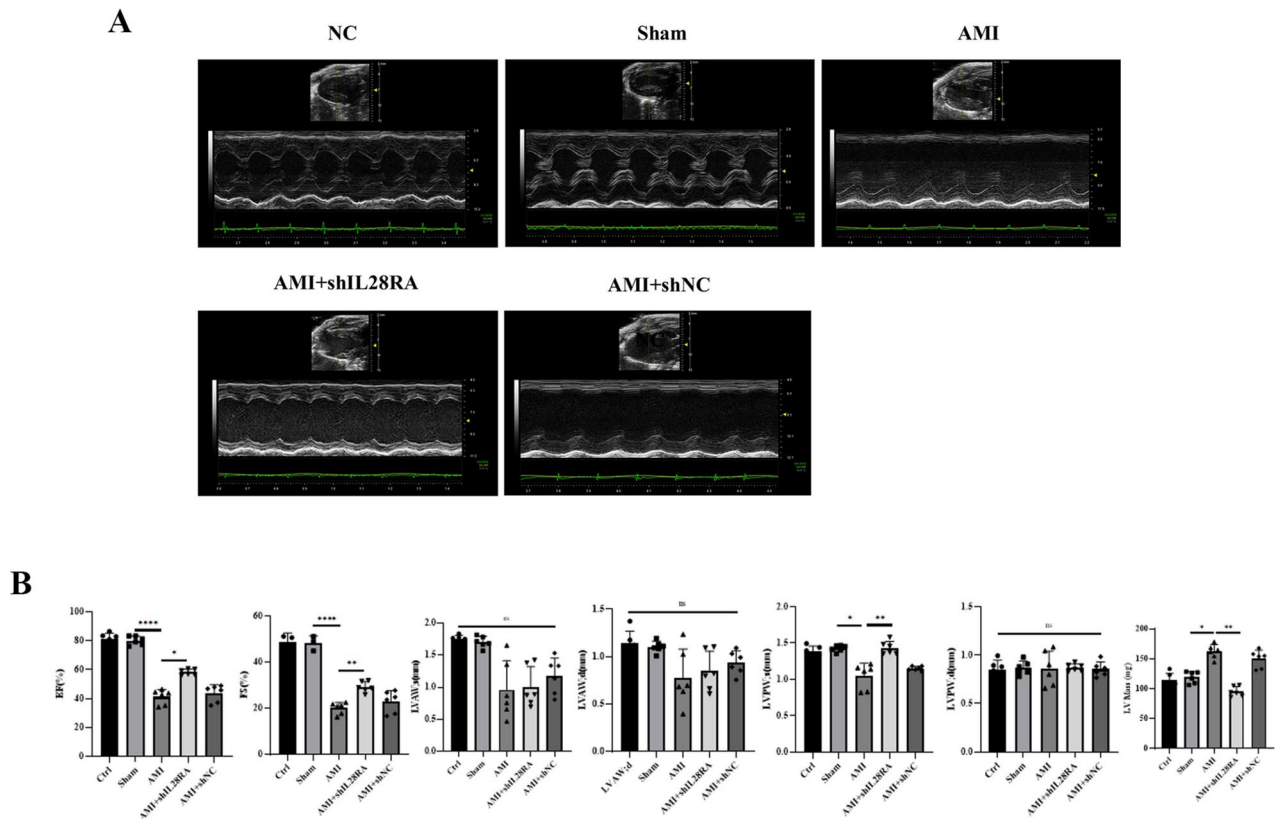
Fig. 4. Heart function, ventricular structure, and weight of mice in five groups were assessed with a focus on presenting the longitudinal sections for analysis. Echocardiograms from each group were found to be representative, and various parameters such as left ventricular ejection fraction (EF%), left ventricular fractional shortening (FS%), left ventricular mass (LV Mass), left ventricular anterior wall thickness at end-diastole and end-systole (LVAW;d, LVAW;s), and left ventricular posterior wall thickness (LVPW;d, LVPW;s) were statistically analyzed. ($^*P < 0.05$, $^{**}P < 0.01$, $^{****}P < 0.0001$).

IL28A-IL28RA induce cardiomyocyte apoptosis by activating JAK1/STAT1 signaling pathway

To further understand the signaling pathways activated by the combination of IL28A/IL28B and IL28RA, we observed a significant increase in the expression of IL28A and IL28RA following AMI ($P < 0.05$). Additionally, the ratios of p-JAK1/JAK1 and p-STAT1/STAT also showed a notable increase ($P < 0.05$). Furthermore, in the AMI + shIL28RA group, there was a significant decrease in the expressions of IL28A and IL28RA compared to the AMI + shNC group, along with a notable decrease in the p-JAK1/JAK1 and p-STAT1/STAT ratios ($P < 0.05$). The expression of IL28B in myocardium did not change significantly in each group ($P > 0.05$) (see Fig. 7 and Supplementary Information 1 and 2).

To evaluate apoptotic cells in cardiomyocytes, we conducted TUNEL staining and assessed the expression of apoptosis-related proteins BAX and Bcl2. Compared to the control group, the acute myocardial infarction (AMI) group exhibited a higher number of TUNEL-positive cells and an elevated BAX/Bcl2 ratio, indicating increased apoptosis. Notably, in comparison to the AMI + shNC group, the AMI + shIL28RA group showed a significant reduction in the number of positive cells, along with a decreased BAX/Bcl2 ratio. These findings suggest that downregulating IL28RA expression in the myocardial infarction area may alleviate apoptosis (see Fig. 8 and Supplementary Information 1 and 2).

Discussion

Although advancements in the treatment of AMI are ongoing, many patients still do not receive optimal treatment in a timely manner, leading to irreversible damage to the heart muscle. While the acute inflammatory response in myocardial infarction has been extensively studied, it is now increasingly recognized that the subsequent adaptive immune response can exacerbate myocardial damage[7]. Excessive tissue necrosis following an AMI can trigger this adaptive immune response, resulting in a significant increase in B cells and T cells in the blood vessels[8]. The prolonged presence of antigen-specific T and B cells may cause sustained low-level tissue damage, cardiomyocyte apoptosis, and eventually heart failure[3]. Adaptive immunity is closely linked to the IL-10 cytokine family, which includes IL-10, IL-19, IL-20, IL-22, IL-24, IL-26, as well as the distantly related IL28A, IL28B, and IL-29[9,10]. Among these, IL-10, known for its anti-inflammatory properties, can help regulate excessive inflammation and reduce damage post-myocardial infarction. In a study involving mice induced with myocardial infarction, those injected with recombinant mouse IL-19 showed reduced infarct size and decreased
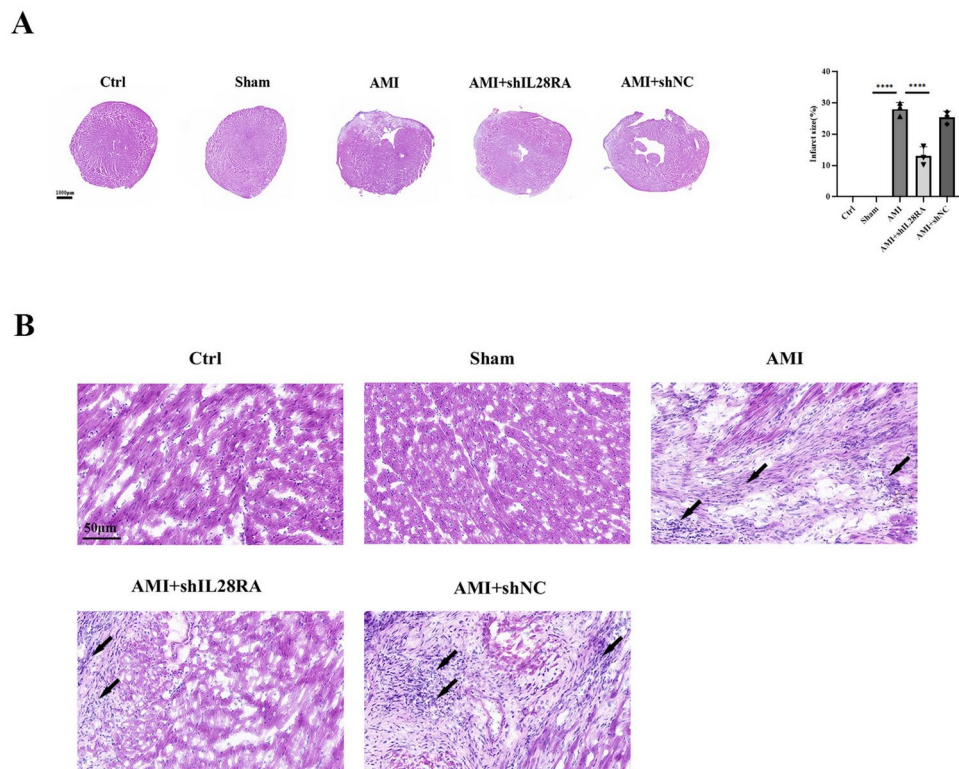
Fig. 5. HE staining was employed to compare the myocardial tissue morphology and infarct area among the five groups of mice. When compared to the control group, the infarct area in the AMI group and the AMI + shNC group exhibited a significant increase, while the infarct area in the AMI + shIL28RA group showed a significant decrease. Both the AMI group and the AMI + shNC group demonstrated marked nuclear pyknosis, cytoplasmic dissolution, and disordered texture (black arrows). However, these pathological features were markedly improved in the AMI + shIL28RA group ($^{****}P < 0.0001$).

cell apoptosis. While upregulation of IL-20 can worsen cardiomyocyte damage, IL-22 plays an indirect role in protecting cardiomyocytes[11].

IL28A and IL28B, newly discovered from human genome sequences, have been the subject of limited research regarding their association with cardiovascular diseases. In this pioneering and interesting study, we evaluated the serum levels of IL28A and IL28B in patients following AMI. Our findings revealed a significant increase in IL28A levels and a notable decrease in IL28B levels post-AMI. This phenomenon could be attributed to the distinct functions of IL28A and IL28B, similar to IL-10, IL-19, IL-20 and IL-22 discussed previously, which exhibit varied roles in myocardial ischemia. Further research is needed to elucidate the specific roles of IL28A and IL28B in this context. Additionally, among patient characteristics and serum indicators, IL28A and IL28B were found to be closely associated with BMI and HDL levels. While TG, TC, LDL and HDL are well-established risk factors for myocardial infarction[12], the specific relationship of IL28A and IL28B with TG, TC, and LDL levels may be influenced by the statins prescribed to the patient. Statins are known to effectively reduce TG, TC, and LDL levels, but their impact on HDL levels remains uncertain[13]. Additionally, obesity is recognized as a risk factor for myocardial infarction, which aligns with the findings of our study.

IL28A, IL28B, and IL-29 are referred to as IFN-λs. These cytokines, secreted by lymphocytes, play a critical role in immune defense at barrier surfaces. Recent research indicates elevated levels of IFN-λs in autoimmune and infectious diseases[14–17]. However, their involvement in AMI is still a topic of debate. IL28RA, the specific receptor for IFN-λ, modulates immune responses in various diseases upon binding with IFN-λ. Studies have shown that hepatocytes, epithelial cells, and salivary gland cells in patients with Sjögren's syndrome express IL28RA and respond directly to IFN-λ, unlike lymphocytes and monocytes[18,19]. IFN-λs signal through common JAK/STAT pathways that are linked to IFN-I, leading to the transcription of IFN-stimulated genes[4,20–22]. Previous studies have demonstrated that inhibiting IL28RA expression in cardiomyocytes reduces apoptosis and protects damaged cells. In this study, we present evidence that binding of IL28A, but not IL28B, to IL28RA induces cardiomyocyte apoptosis via the JAK1/STAT1 pathway.

The research findings suggest that IL28RA may have distinct roles in the development of AMI. Previous studies have demonstrated that immune cells like dendritic cells and neutrophils express IL28RA. In the context of psoriasis, IL28RA has been shown to inhibit cell proliferation by halting cell cycle progression, making it a potential target for treating psoriasis[23]. In individuals with inflammatory bowel disease and in mouse models, there is a notable increase in IL28RA expression. Research involving IL28RA-knockout mice with colitis and control groups has revealed that the administration of IL28RA can enhance mucosal healing[24]. Additionally,
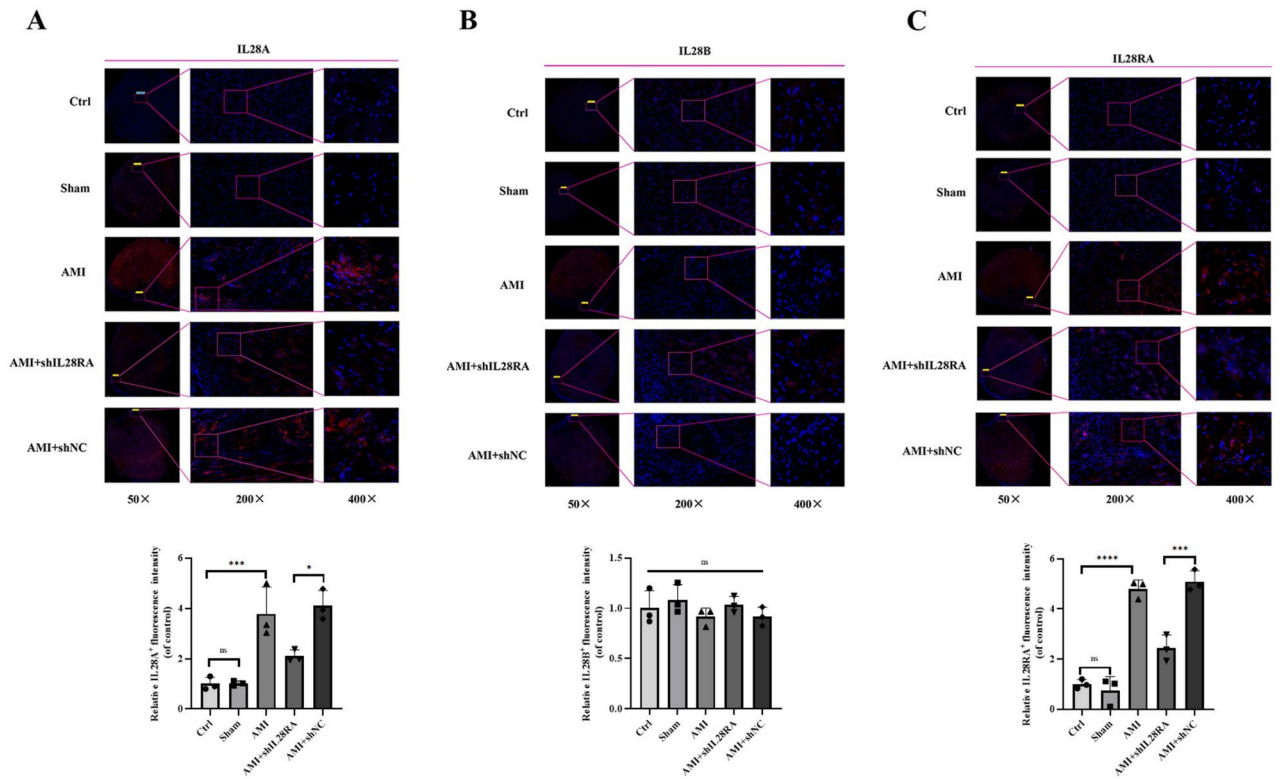
Fig. 6. Immunofluorescence images of IL28A, IL28B, and IL28RA expression in mouse heart tissue were presented. In comparison to the control group, the expression levels of IL28RA and IL28A were significantly elevated in the AMI group. Conversely, the expression levels of IL28RA and IL28A in the AMI + shIL28RA group were significantly reduced when compared to the AMI group. Importantly, no significant differences in IL28B expression were observed among the groups. ($^*P < 0.05$, $^{***}P < 0.001$, $^{****}P < 0.0001$).
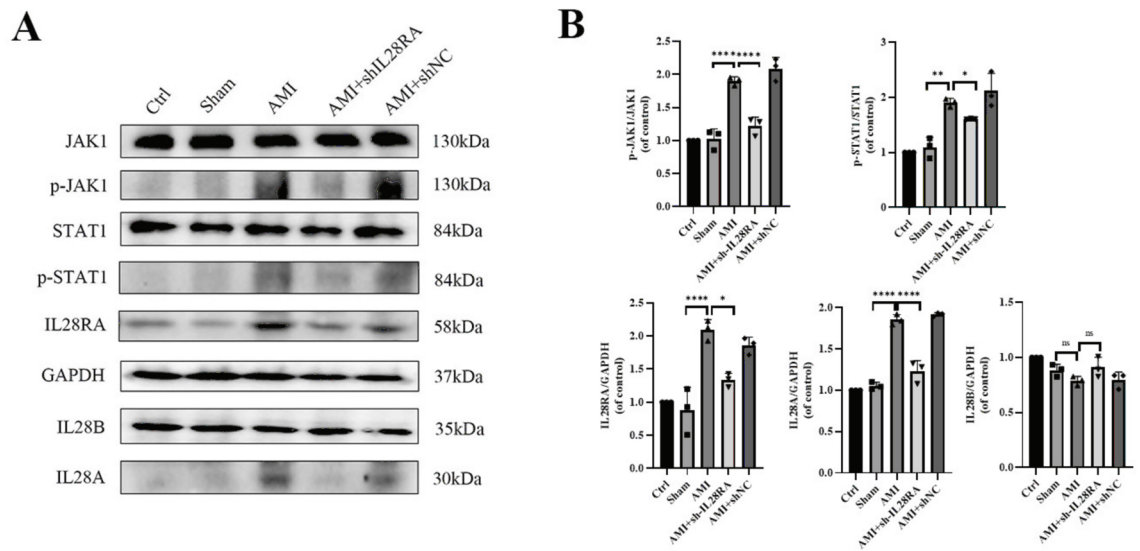

Fig. 7. Western blot analysis demonstrated the expression levels of JAK1, p-JAK1, STAT1, p-STAT1, IL28A, IL28B, and IL28RA in mouse heart tissue. Compared to the control group, the expression levels of p-JAK1/ STAT1, p-STAT1/STAT1, IL28A, and IL28RA were significantly elevated in the AMI group. In contrast, the expression levels of p-JAK1/STAT1, p-STAT1/STAT1, IL28A, and IL28RA were significantly reduced in the AMI + shIL28RA group compared to the AMI group. No significant differences were observed in IL28B between the groups. ($^*P < 0.05$, $^{**}P < 0.01$, $^{****}P < 0.0001$).

A

B
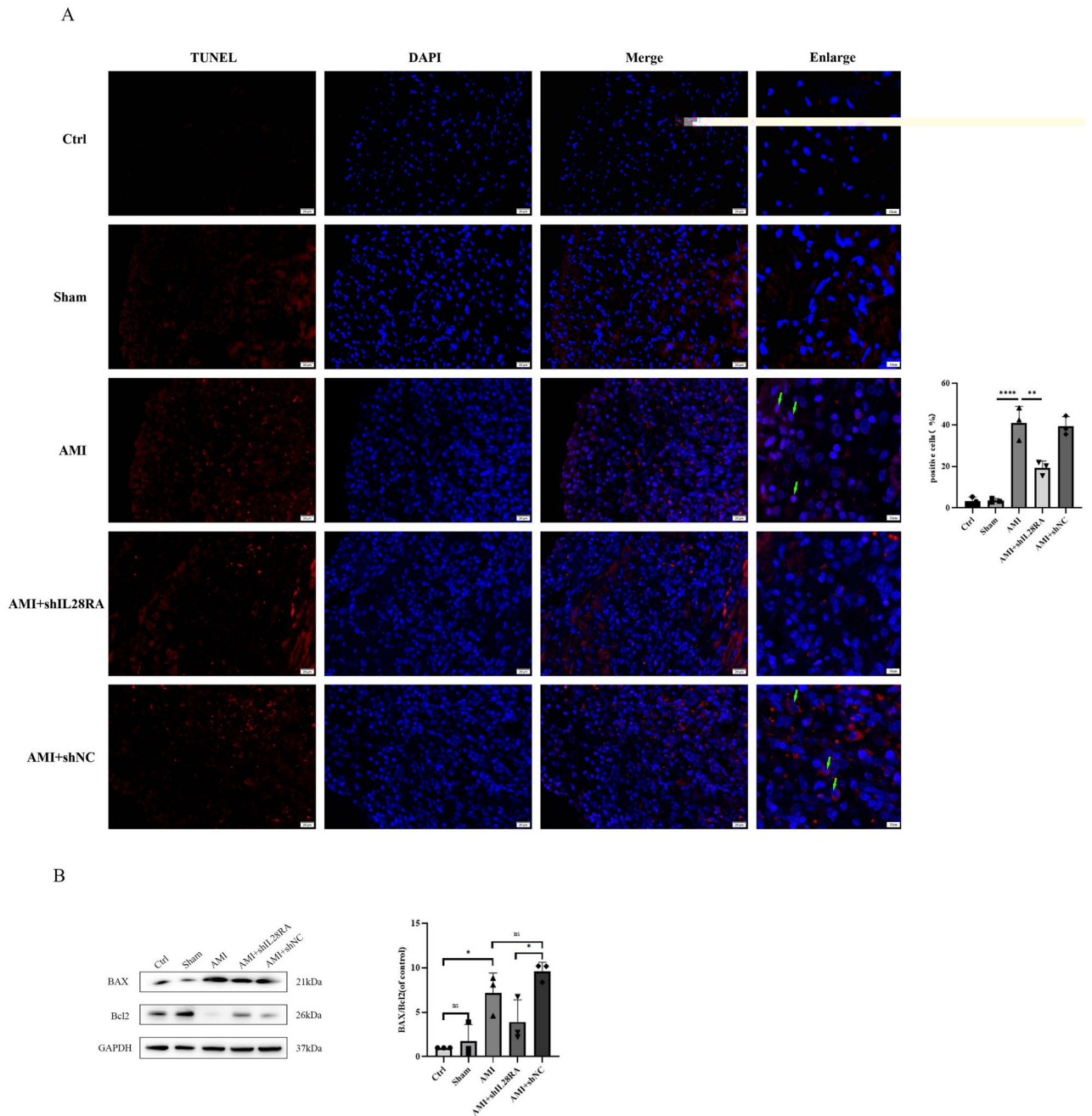
Fig. 8. Cell apoptosis rate of TUNEL staining of heart tissues of the five groups of mice was evaluated. In comparison to the control group, there was a significant increase in TUNEL staining-positive cells in the AMI group. Conversely, the AMI + shIL28RA group exhibited a significant decrease in positive cells compared to the AMI group (**A**). The BAX/Bcl2 ratio was utilized to assess cardiomyocyte apoptosis. Apoptosis levels in the AMI group were significantly higher than those in the Ctrl group, while the AMI + shIL28RA group exhibited reduced apoptosis compared to the AMI + shNC group (**B**). ($^{*}P < 0.05$, $^{**}P < 0.01$, $^{****}P < 0.0001$).

the IL28RA gene is implicated in cardiovascular diseases. In a mouse model of induced cardiomyopathy using low-dose chlorpromazine, researchers observed a significant rise in IL28RA gene expression and cardiomyocyte apoptosis in myocardial tissue after continuous administration of low-dose chlorpromazine for 3 weeks[25]. In our previous study, high-throughput screening of patients with myocardial infarction identified elevated expression of the IL28RA gene. Subsequent cell experiments confirmed that silencing the IL28RA gene could effectively protect myocardial cells from hypoxia-reoxygenation and decrease cell apoptosis. Our findings suggest a potential link between the IL28RA gene, promotion of cardiomyocyte apoptosis, and myocardial injury. However, these studies did not specifically investigate the response of IL28A, IL28B, and IL28RA following AMI.

To further explore the impact of IL28A and IL28B on cardiomyocytes post-AMI and the mechanism of cardiomyocyte apoptosis triggered by their interaction with IL28RA, an AMI mouse model was established.
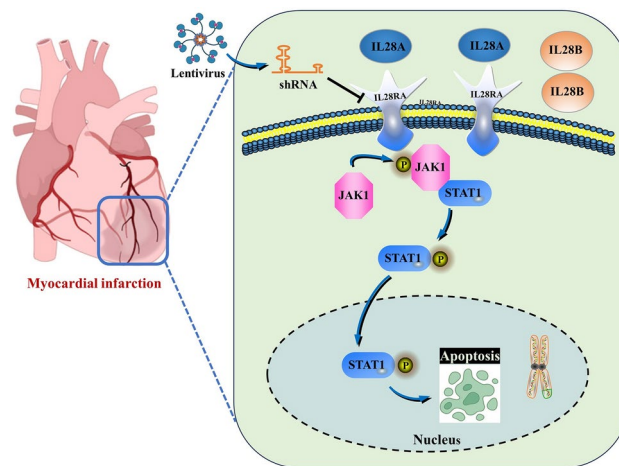
Fig. 9. Graphic summary. Following acute myocardial infarction, the level of IL28A in mouse myocardial tissue increased significantly, while the level of IL28B did not show a significant increase. Concurrently, the level of IL28RA also significantly increased, leading to phosphorylation activation of the JAK1/STAT1 pathway and subsequent apoptosis induction. Knocking down IL28RA reversed these changes.

The success of the AMI model was validated through TTC staining and echocardiography. A significant upregulation of IL28A and IL28RA expression was observed in the myocardial infarction tissue, as validated through immunofluorescent staining and Western blot analysis. Furthermore, there was an increase in the levels of proteins linked to the JAK1/STAT1 signaling pathway, which was associated with heightened cardiomyocyte apoptosis. Previous studies have indicated that reducing IL28RA expression at the cellular level can effectively inhibit cardiomyocyte apoptosis[5,6]. In this investigation, mice with AMI were used to assess the impact of downregulating IL28RA expression in vivo. The results revealed a significant enhancement in cardiac function, ventricular structure, and ventricular hypertrophy in the mice. Similar to type IFN-I, IFN-λ exerts its effects through the JAK/STAT signaling pathway, contributing to antiviral activity and immune response activation[26,27]. These findings suggest that IL28A, rather than IL28B, may impact cardiomyocytes post-myocardial infarction by binding to IL28RA and inducing apoptosis through the phosphorylated JAK1/STAT1 signaling pathway activation (see Fig. 9).

In our study, we noted a significant decrease in IL28B levels in the serum of patients following AMI. However, animal experiments did not reveal substantial changes in IL28B expression in myocardial tissue in myocardial infarction models. Unfortunately, our study did not assess the levels of IL28A and IL28B in mouse serum, which may explain the observed discrepancies. These differences could be attributed to interspecies variations or variations in the timing of serum index detection between patients and mice with myocardial infarction. We hypothesize that following myocardial infarction, IL28A specifically interacts with IL28RA on cardiomyocytes, while IL28B may primarily affect blood flow. Presently, IL28A and IL28B are predominantly investigated in the context of viral hepatitis, with limited exploration of their connection to cardiovascular disease. This underscores the necessity for further comprehensive investigation in future research.

The specific mechanism of IL28A and IL28B function after myocardial infarction, as well as the potential protective effect of IL28RA gene deficiency in myocardial injury post-myocardial infarction, remains unexplored in our research. Future studies involving animal experiments with IL28RA gene knockout mice could provide valuable insights into how inhibiting IL28RA gene expression may offer protection against myocardial injury following myocardial infarction. Investigating the novel role of adaptive immunity in myocardial infarction over a longer timeframe could offer further understanding and potentially hasten the development of new therapeutic approaches. Continued research in this field will undoubtedly enhance our comprehension of the intricate immune responses and their implications on cardiac function in the context of myocardial infarction.

Data availability
The datasets used and/or analysed during the current study available from the corresponding author on reasonable request.

References
1. Santos-Zas, I., Lemarié, J., Tedgui, A. & Ait-Oufella, H. Adaptive immune responses contribute to post-ischemic cardiac remodeling. *Front. Cardiovasc. Med.* **5**, 198. https://doi.org/10.3389/fcvm.2018.00198 (2018).
2. Xu, Y. et al. Bone marrow-derived naïve B lymphocytes improve heart function after myocardial infarction: A novel cardioprotective mechanism for empagliflozin. *Basic Res. Cardiol.* **117**(1), 47. https://doi.org/10.1007/s00395-022-00956-1 (2022).
3. Hofmann, U. & Frantz, S. Role of lymphocytes in myocardial injury, healing, and remodeling after myocardial infarction. *Circ. Res.* **116**(2), 354–367. https://doi.org/10.1161/circresaha.116.304072 (2015).

4. Manivasagam, S. & Klein, R. S. Type III interferons: Emerging roles in autoimmunity. *Front. Immunol.* **12**, 764062. https://doi.org/10.3389/fimmu.2021.764062 (2021).
5. Gong, G. et al. Protective effects of IL28RA siRNA on cardiomyocytes in hypoxia/reoxygenation injury. *Anatol. J. Cardiol.* **18**(3), 168–174. https://doi.org/10.14744/AnatolJCardiol.2017.7763 (2017).
6. Gong, G. et al. IL28RALncRNA260-specific siRNA targeting gene inhibit cardiomyocytes hypoxic/reoxygenation injury. *J. Thorac. Dis.* **9**(8), 2447–2460. https://doi.org/10.21037/jtd.2017.07.07 (2017).
7. Forte, E. et al. Cross-priming dendritic cells exacerbate immunopathology after ischemic tissue damage in the heart. *Circulation* **143**(8), 821–836. https://doi.org/10.1161/circulationaha.120.044581 (2021).
8. Adamo, L., Rocha-Resende, C., Prabhu, S. D. & Mann, D. L. Reappraising the role of inflammation in heart failure. *Nat. Rev. Cardiol.* **17**(5), 269 (2021).
9. Wei, W., Zhao, Y., Zhang, Y., Jin, H. & Shou, S. The role of IL-10 in kidney disease. *Int. Immunopharmacol.* **108**, 108917. https://doi.org/10.1016/j.intimp.2022.108917 (2022).
10. Ni, S., Shan, F. & Geng, J. Interleukin-10 family members: Biology and role in the bone and joint diseases. *Int. Immunopharmacol.* **108**, 108881. https://doi.org/10.1016/j.intimp.2022.108881 (2022).
11. Xu, S. et al. The role of interleukin-10 family members in cardiovascular diseases. *Int. Immunopharmacol.* **94**, 107475. https://doi.org/10.1016/j.intimp.2021.107475 (2021).
12. Salinero-Fort, M. A. et al. Cardiovascular risk factors associated with acute myocardial infarction and stroke in the MADIABETES cohort. *Sci. Rep.* **11**(1), 15245. https://doi.org/10.1038/s41598-021-94121-8 (2021).
13. Lu, Y. et al. Sex differences in lipid profiles and treatment utilization among young adults with acute myocardial infarction: Results from the VIRGO study. *Am. Heart J.* **183**, 74–84. https://doi.org/10.1016/j.ahj.2016.09.012 (2017).
14. Strine, M. S. et al. Tuft-cell-intrinsic and -extrinsic mediators of norovirus tropism regulate viral immunity. *Cell Rep.* **41**(6), 111593. https://doi.org/10.1016/j.celrep.2022.111593 (2022).
15. Wang, Y. F. et al. Identification of shared and Asian-specific loci for systemic lupus erythematosus and evidence for roles of type III interferon signaling and lysosomal function in the disease: A multi-ancestral genome-wide association study. *Arthritis Rheumatol.* **74**(5), 840–848. https://doi.org/10.1002/art.42021 (2022).
16. Chiriac, M. T. et al. Activation of epithelial signal transducer and activator of transcription 1 by interleukin 28 controls mucosal healing in mice with colitis and is increased in mucosa of patients with inflammatory bowel disease. *Gastroenterology* **153**(1), 123–138. https://doi.org/10.1053/j.gastro.2017.03.015 (2017).
17. Mallampalli, R. K. et al. Interferon lambda signaling in macrophages is necessary for the antiviral response to influenza. *Front. Immunol.* **12**, 735576. https://doi.org/10.3389/fimmu.2021.735576 (2021).
18. Dickensheets, H., Sheikh, F., Park, O., Gao, B. & Donnelly, R. P. Interferon-lambda (IFN-λ) induces signal transduction and gene expression in human hepatocytes, but not in lymphocytes or monocytes. *J. Leukocyte Biol.* **93**(3), 377–385. https://doi.org/10.1189/jlb.0812395 (2013).
19. Ha, Y. J. et al. Increased expression of interferon-λ in minor salivary glands of patients with primary Sjögren's syndrome and its synergic effect with interferon-α on salivary gland epithelial cells. *Clin. Exp. Rheumatol.* (3), 31–40 (2018).
20. Zanoni, I., Granucci, F. & Broggi, A. Interferon (IFN)-λ takes the helm: Immunomodulatory roles of type III IFNs. *Front. Immunol.* **8**, 1661. https://doi.org/10.3389/fimmu.2017.01661 (2017).
21. Kolářová, L. et al. De novo developed protein binders mimicking Interferon lambda signaling. *FEBS J.* **289**(9), 2672–2684. https://doi.org/10.1111/febs.16300 (2022).
22. Wells, A. I. & Coyne, C. B. Type III interferons in antiviral defenses at barrier surfaces. *Trends Immunol.* **39**(10), 848–858. https://doi.org/10.1016/j.it.2018.08.008 (2018).
23. Yin, X., Zhang, S., Li, B., Zhang, Y. & Zhang, X. IL28RA inhibits human epidermal keratinocyte proliferation by inhibiting cell cycle progression. *Mol. Biol. Rep.* **46**(1), 1189–1197. https://doi.org/10.1007/s11033-019-04586-0 (2019).
24. Chiriac, M. et al. Activation of epithelial signal transducer and activator of transcription 1 by interleukin 28 controls mucosal healing in mice with colitis and is increased in mucosa of patients with inflammatory bowel disease. *Gastroenterology* **153**(1), 123-138.e8. https://doi.org/10.1053/j.gastro.2017.03.015 (2017).
25. Tsai, C., Ikematsu, K., Sakai, S., Matsuo, A. & Nakasono, I. Expression of Bcl2l1, Clcf 1, IL-28ra and Pias1 in the mouse heart after single and repeated administration of chlorpromazine. *Legal Med. (Tokyo, Japan)* **13**(5), 221–225. https://doi.org/10.1016/j.legalmed.2011.04.006 (2011).
26. Chyuan, I., Tzeng, H. & Chen, J. Signaling pathways of type I and type III interferons and targeted therapies in systemic lupus erythematosus. *Cells* https://doi.org/10.3390/cells8090963 (2019).
27. Yin, Y., Ma, J., Van Waesberghe, C., Devriendt, B. & Favoreel, H. Pseudorabies virus-induced expression and antiviral activity of type I or type III interferon depend on the type of infected epithelial cell. *Front. Immunol.* **13**, 1016982. https://doi.org/10.3389/fimmu.2022.1016982 (2022).

Author contributions
GG and XXC completed the experimental content and wrote the draft paper. GG and XHZ drew pictures. JY and WHW planned the study and modified the article. All authors gave the final approval and agreed to be accountable for all aspects of the work. All authors read and approved the final manuscript.

Declarations

Competing interests
The authors declare no competing interests.

Ethical approval

The study protocol was approved by the Ethical Committee of Jinling Hospital (2023JLHGZRDWLS-00013) and the Ethical Committee provided consent to access the medical records. This study is reported in accordance with ARRIVE guidelines.

Additional information

Supplementary Information The online version contains supplementary material available at https://doi.org/10.1038/s41598-024-83668-x.

Correspondence and requests for materials should be addressed to J.Y. or W.W.

Reprints and permissions information is available at www.nature.com/reprints.

Publisher's note Springer Nature remains neutral with regard to jurisdictional claims in published maps and institutional affiliations.